Chapter 6

Role of Graphene in Photocatalytic Solar Fuel Generation

Babak Adeli and Fariborz Taghipour

Additional information is available at the end of the chapter

http://dx.doi.org/10.5772/intechopen.72623

Abstract

One of the most promising methods for conversion and storage of solar energy is in the form of the chemical bonds of an energy carrier, such as hydrogen or light hydrocarbons. However, the traditional methods to harness and store solar energy are simply too expensive to be implemented on a large scale. It has been documented that the recombination of photo-induced charge carriers is the greatest source of inefficiency in photocatalytic systems. In the last decade, graphene derivatives and their functionalized nanostructures were extensively utilized for various roles to improve the efficiency of photocatalytic solar fuel generation. These include photocatalyst/redox active sites via band gap and defect density engineering, charge acceptor due to their excellent carrier mobility, a solid-state charge mediator by electronic band alignment, and light absorber by taking advantage of their photoluminescence characteristics at the nanoscale. This chapter aims to provide an authoritative and in-depth review on the properties and application of graphene derivatives, as well as the recent advances in the design of graphene-based photocatalytic systems. The knowledge extracted from the presented materials can be applied to other applications dealing with surface chemistry, interfacial science, and optoelectronic device fabrication.

Keywords: solar fuel generation, graphene, photocatalyst, water splitting, CO_2 reduction

1. Introduction

Direct production of fuels from sunlight is an attractive route to address the energy crisis facing humanity in the twenty-first century, because it inherently provides a method for extracting energy during the night and for cost-effectively dispatching and distributing energy in the existing infrastructure for use in the residential, industrial, and transportation sectors [1]. That places the photocatalytic splitting of water and the conversion of carbon dioxide (CO_2) to light

hydrocarbons, driven solely by sunlight, among the most promising approaches. These were studied extensively in the last decade [2]. However, visible-light water splitting and CO_2 reduction are inherently associated with inefficiencies and complicated processes. For instance, the possible products of these processes may include H_2, HCOOH, HCHO, CH_3OH, CO, and CH_4, which are selective and dependent on many competing factors (e.g., reaction kinetics, redox potentials of photo-induced charge carriers, morphology, crystalline structure, exposed crystalline facets and the surface properties of the utilized photocatalyst, and redox active sites) [3]. In addition, the energy levels of the photo-induced charges are relative to the electronic band structure of the employed semiconductor; thus, the desired photocatalyst must possess a matching molecular orbital structure corresponding to the redox potentials of the reaction. Electrons contain the energy of the lowest unoccupied molecular orbital (LUMO) and holes pose the potential energy of the highest occupied molecular orbital (HOMO). These energy levels are also known as the bottom of the semiconductor's conduction band (CB) and the top of the semiconductor's valence band (VB) and are shown in **Figure 1**. For a photocatalytic reaction to proceed, the photo-induced charges must pose a suitable energy level corresponding to redox potential of the reaction. Taking the solar water-splitting reaction as an example, the photo-excited electrons and the holes must contain more negative and more positive energy compared to the water reduction (0 eV vs. NHE) and the water oxidation potential (1.23 eV vs. NHE), respectively. Upon photo-excitation and the generation of photo-induced electrons and holes, the charge carriers can reach to the electrolyte and participate in redox reactions at CB and VB, as demonstrated in **Figure 1**.

Despite the efforts in utilizing metal oxide, sulfide, and nitride photocatalysts, as well as their binary and ternary solid solutions, the efficiencies of the solar fuel generation processes have

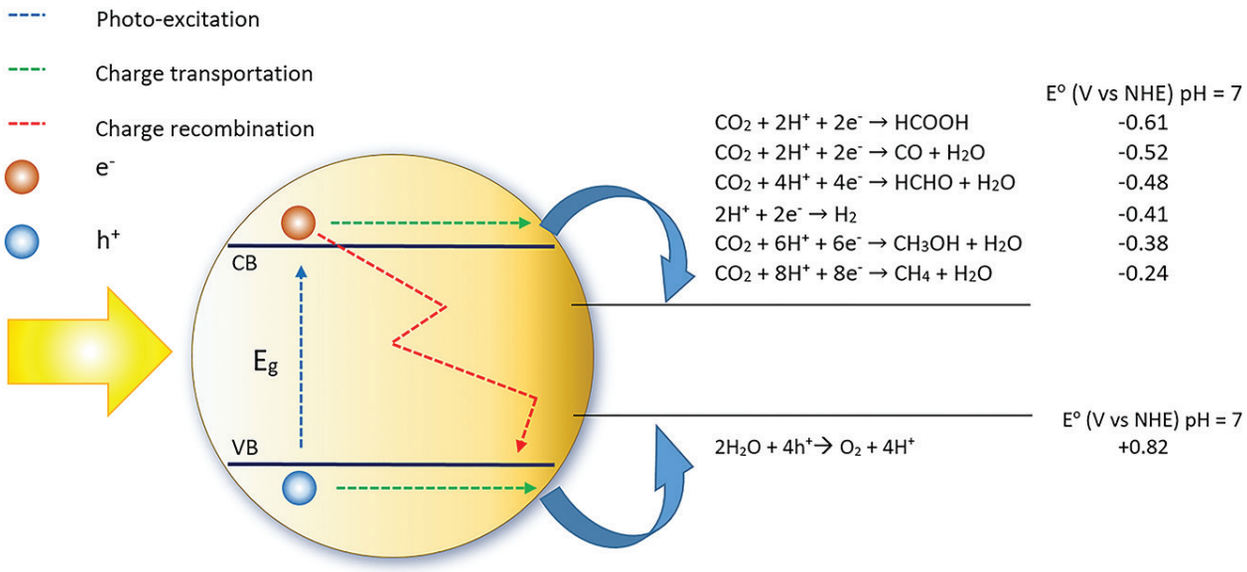

Figure 1. Band gap energy (E_g), valence band (VB), and conduction band (CB) potential of semiconductors. The figure also shows processes (photo-excitation, charge transportation, and charge recombination) that occur upon striking the surface of a semiconductor by a light photon with energy greater than the semiconductor's band gap. Once photo-induced charges reach the surface of the semiconductor, several possible products can proceed (i.e., water splitting and CO_2 conversion). The potential of the redox reactions is denoted by E^o.

remained too low for them to be feasibly commercialized. Such inefficiencies are primarily attributed in the recombination of photo-induced charges, displayed by red dashed-line in **Figure 1**, which occurs mainly at the grain boundaries and the crystalline defects within the bulk of photocatalyst, where the diffusion path of charge carriers is considerable, and/or the density redox active sites are not sufficient [4]. In the last few years, various strategies—emphasizing the nanoscale morphology and exposed crystallographic facets, as well as increasing the specific surface area and the number of redox active sites—have led to outstanding improvements. However, these are not enough to put the commercialization of solar water splitting and CO_2 reduction in sight. Moreover, the abundance of photocatalyst materials and fabrication routes of advance structures has hindered further consideration of some candidate materials.

In the last decade, carbon-based materials, such as carbon nanotubes (CNTs), graphene, graphene oxide, carbon quantum dots, carbon fibers, activated carbon, and carbon black, have been the focus of intense research, owing to their peculiar characteristics, such as tunable electronic band structure, ultra-high specific surface area, tailored crystalline structure, and reactive crystallographic facets. Among them, graphene derivatives have grasped researchers' attention, due to their effectiveness as redox active sites, tunable defect-density active sites, short carrier's diffusion paths, and high electron mobility, as well as efficient light harvesting within their two-dimensional (2D) crystallography.

Over 18,000 articles related to graphene were published from 2004 to 2014. In the last decade, due to the advances in materials sciences and nanotechnology, tailoring the optical, structural, and electrochemical characteristics of graphene-based photocatalysts at the nanoscale toward quantum efficiency (QE) improvement has been extensively studied. This chapter aims to present the recent advances in the application of graphene-based materials in solar fuel generation via water splitting and CO_2 conversion. Readers are encouraged to reach out to comprehensive review articles previously published on topics related to the subject of this chapter [3, 5–9].

2. Graphene derivative materials

Dating back to October 2004, a revolution in science and technology was triggered when Novoselov et al. [10] had prepared stable 2D sheets of carbon atoms at ambient conditions, the so-called graphene nanosheets. Graphene, as an allotrope of carbon, is an isolated monolayer sheet containing atoms that are tightly packed into an sp^2 honeycomb lattice hybridized C—C bond with a π-electron cloud and is considered as one of the most important materials in the current century. Graphene soon became one of the attractive components in photonic device fabrication, fuel conversion, fuel storage, environment, sensing, and catalysis, owing to its outstanding mechanical, thermal, optical, and electrical properties. Photocatalytic applications, highly conductive graphene nanosheets (2D) and quantum dots (zero-dimensional) with a massive surface area and ultra-active catalytic facets, particularly on the dangling crystallography edges, are excellent materials for hybridization with prominent photocatalysts to enhance the separation of photo-excited charges and the active surface area for the redox reactions.

Early studies showed that monolayer graphene can be successfully isolated and studied; while a 2D crystalline graphene nanosheet is known to be thermodynamically unstable, its properties are not yet well known [11]. Graphene is a zero band gap semimetal with a small overlap between its HOMO and LUMO [12–14]. In fact, the electrical, mechanical, optical, and thermal properties of graphene are very similar to those of single-walled carbon nanotubes (SWCNTs), while it can be prepared at significantly lower cost [11]. In particular, graphene's massive theoretical specific surface area (~2600 $m^2 g^{-1}$ [15]), high mobility of charge carriers (~10,000 $cm^2 V^{-1} s^{-1}$ at room temperature, approaching to 200,000 $cm^2 V^{-1} s^{-1}$ for lower carrier densities and temperatures [16]), plus its excellent thermal conductivity (3000–5000 $W m^{-1} K^{-1}$ [17]), 97.7% optical transmittance, and <0.1% reflectance [18] (monolayer graphene nanosheet) make it an excellent choice for light harvesting and the fabrication of energy conversion devices [15, 16, 19].

Within a few years, graphene-derivative materials, such as graphene oxide (GO), reduced graphene oxide (rGO), nanoribbons, quantum dots (QDs), and their functionalized nanostructures, demonstrated even more exciting characteristics. GO is a 2D carbon nanomaterial with many merits, such as low manufacturing cost, facile mass production, fascinating chemistry, and remarkable semiconducting behavior [5, 20–25]. The oxygen-containing functional groups on the surface of GO make it readily dispersed in aqueous solutions and effectively interact with other organic and inorganic compounds, as well as ionic species [26]. The surface of GO nanosheets is mainly decorated with epoxide (═O) and hydroxyl (─OH) groups, while small composition of carbonyl (─C═O) and carboxyl (─COOH) groups are linked to the nanosheet's edges [27]. These oxygen functionalities allow GO and rGO to interact with a wide range of precursors and structures through noncovalent, covalent, and/or ionic interactions [15, 18]. In addition, various densities of sp^3 hybridization in the GO structure create a wide range of interesting characteristics. Unlike sp^2 hybridization, which is attributed to the bonding of carbon atoms to the neighboring carbon atoms (which are not connected with hydroxy or epoxy groups) or oxygen in the form of carbonyl or carboxyl groups, sp^3 hybridization forms when carbon atoms are bonded to epoxy or hydroxyl groups [28–30]. Density functional theory (DFT) studies, in agreement with experimental observations, confirm the role of oxygen functional groups on the optical properties of graphene over a wide range [29–31]. An intense blue shift in the electron energy loss spectrum (EELS) of GO was observed when the concentration of epoxy and hydroxyl functional groups increased [29, 30]. Interestingly, an increase in the density of carbonyl groups affects the GO EELS; as such, at O/C ~37.5% a red shift about 1.0 eV compared to the pristine graphene is observed [29]. Therefore, the density of surface functionalities can be precisely tuned to control the optical and electrochemical properties of graphene derivatives over a wide range.

QDs, a multilayer zero-dimensional structure, contain sp^2 hybridized honeycomb carbon, have attracted enormous attention, and have been extensively studied for a wide range of applications—energy conversion in particular [32, 33]. Within their ultra-small sizes (typically less than 100 nm), their optical and electronic properties can be tailored, and a well-defined band gap can be formed [34]. Therefore, graphene QDs are like highly crystalline inorganic semiconductor QDs with superior physically and chemically reactive facets [32].

http://dx.doi.org/10.5772/intechopen.72623

3. Role of graphene in solar fuel generation

The improvements in the efficiencies of graphene-based photocatalyst are likely the outcome of these various functionalities and cannot be attributed to one individual phenomenon. In the following sections, the role of graphene derivatives in visible light-driven fuel generation is discussed, and examples from literature are presented.

3.1. Graphene as photocatalyst

There are a handful of materials that can carry out visible light solar fuel generation reaction, exhibiting properties such as short band gap to harvest visible light, and suitable band-edge potential corresponding to redox potentials must be formed within the photocatalyst crystallography. Even then, the photo-generated charges must diffuse through a highly crystalline structure and interact with molecules and ions at highly reactive surface sites. Favorably, graphene as an abundant and cost-effective compound, is among the few nonmetallic photocatalysts that meet all the required conditions.

The molecular energy state of carbon is unique and contains $1s^2$, $2s^2$, and $2p^2$ orbitals, which contribute accordingly in various crystalline structures. As displayed in **Figure 2a**, the sp^2 hybridized structure is formed from s, p_x, and p_y orbitals on each carbon atom connected to the surrounding atoms through three strong covalent σ bonds. In this structure, the remaining $2p_z$ orbital, perpendicular to the graphene plane, overlapped with the one in the neighboring atoms, creating delocalized π (fill band) and π^* (empty band) orbitals, which are also known as graphenes VB and CB [35, 36].

The Fermi level in pristine graphene is located at the points connecting the valence and conduction bands in momentum space, as shown in **Figure 2b**, which is also known as the Dirac point [36]. Graphene exhibits an intrinsic n-type character [38]. Because of a small overlap between its valence and conduction bands, graphene has been characterized as a semimetal and/or a

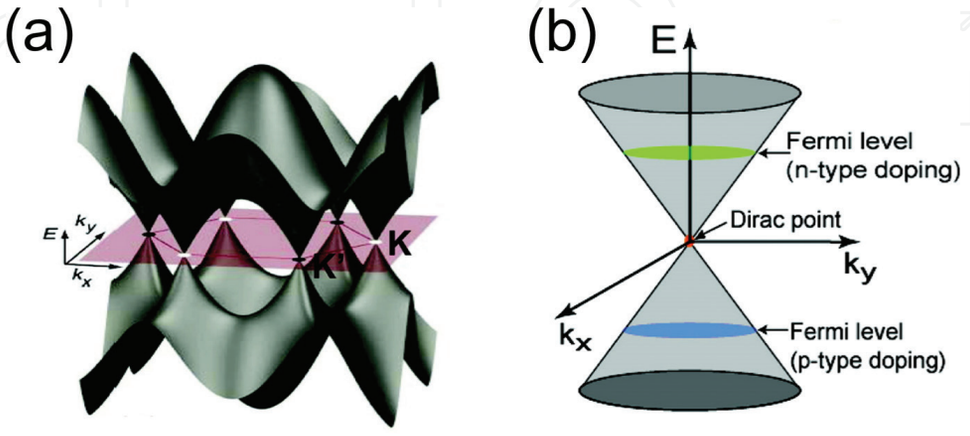

Figure 2. (a) The 3D band structure of graphene. (b) The linear dispersion and the band structure at the Dirac point in graphene [37]. Reprinted with permission from [37]. Copyright 2010 American Chemical Society.

semiconductor with zero band gap energy [13, 39, 40]. This orbital structure creates high conductivity greater than that for silver, which is the least resistive metallic material [41].

By negative and positive doping of graphene's lattice, the state of the Fermi level around the Dirac point can be tuned; therefore, the electronic characteristics of graphene can be tailored. This unique characteristic is attributed to the increase in the concentration of charge carriers by two orders of magnitude, to obtain n- or p-type graphene [17, 35]. For instance, the Fermi level of graphene can be shifted below the Dirac point so p-type characteristics can be formed between graphene and the rutile TiO_2 (110) surface, whereas the holes are accumulated on graphene and electrons are localized in the CB energy state of TiO_2 [38]. Therefore, the graphene electronic structure can be considered a photocatalyst design enabler, as the nanoscale p-n junction can be formed between localized p- and n-doped islands within the 2D crystallography.

From defect-free monolayer graphene to 3D aggregates of multilayer graphene, graphene nanoribbons, rGO, and finally GO, the band gap can be tuned within a wide range through engineering the morphology of the synthesized sample or surface modifications with functional groups. For instance, graphene nanoribbons are 1–100 nm wide, long strips of graphene, where a band gap is formed in the band structure of nanoribbon graphene when the width of the strips is reduced to less than 20 nm [42]. Due to such strange characteristics, graphene nanoribbons, nanomesh, and quantum dots exhibit semiconducting behavior with a band gap less than 0.5 eV [36]. Another strategy to engineer the band gap of graphene derivatives is intermolecular hybridization. An increase in the conductivity of graphene as a result of incorporation with another carbon compound was reported. For example, graphene derivatives–carbon nanotube composites, which are promising materials for transparent conductive materials, exhibited reduced surface resistance from their original 660 Ω sq.$^{-1}$ and 890 Ω sq.$^{-1}$ for rGO, and multiwalled CNTs, respectively, to ~100 Ω sq.$^{-1}$ for the hybrid, although hybridization reduces the optical transmittance of the composite [43]. Similar observations were also reported for CNTs grown on graphene utilized for optoelectronic applications [44–46].

Owing to its large band gap, GO is characterized as an insulating material. Optical measurements of the carriers' lifetime in various wavelengths show an ns-scale decay, indicating semiconducting behavior of GO [47]. Chemical, electrochemical, and photo-induced reduction of GO to rGO are facile and functional routes to tune the band gap of semiconducting nanosheet-like compounds over a wide range, with conductivity up to 30,000 Sm^{-1} [30, 47]. Mathkar et al. [48] studied the controlled reduction of GO using hydrazine vapor while monitoring the optical and compositional properties of the obtained rGO. They successfully controlled the band gap of rGO from 3.5 eV (sp^3 rich) to 1.0 eV (sp^2 rich), as demonstrated in **Figure 3a**.

A similar transition pattern was reported by Mattevi et al. [49] who investigated the surface composition and structure of GO at various stages of thermal reduction. As presented in **Figure 3b**, functionality was developed between the density of sp^2 bonds and the reduction-deriving force (reduction temperature) that exhibited the transformation of an individual GO nanosheet to rGO with a variety of electronic properties. Taking this transition pattern into

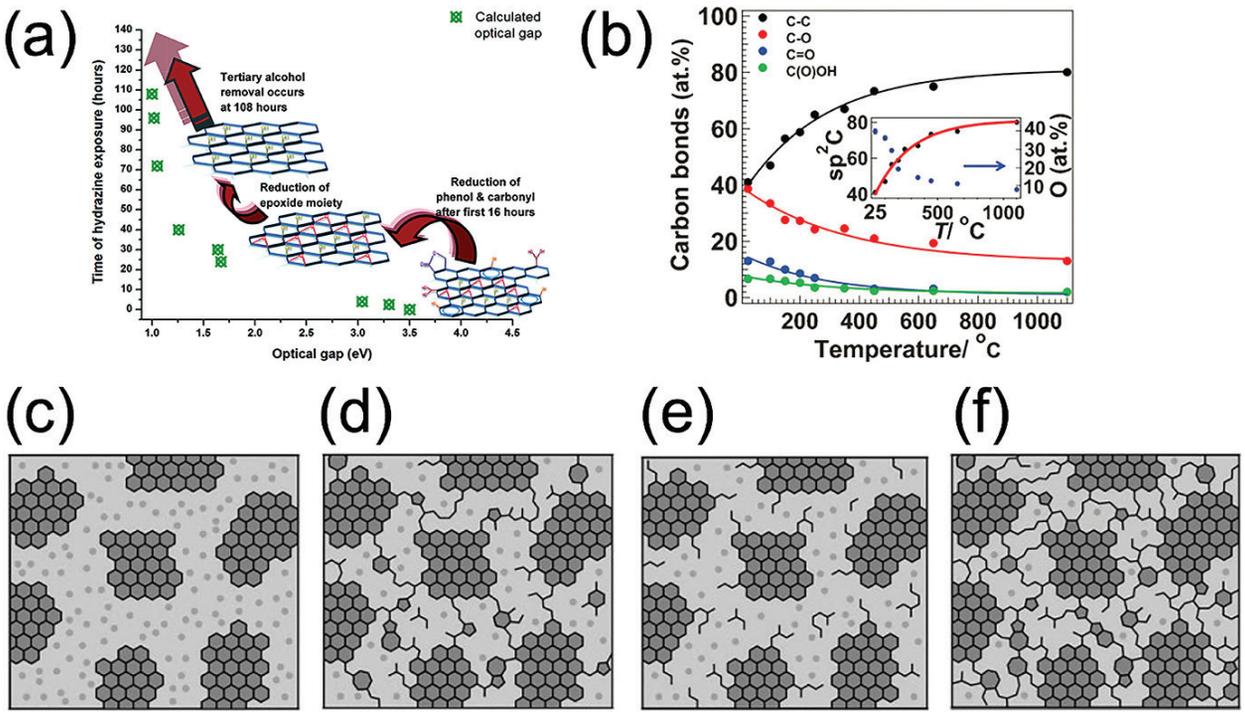

Figure 3. (a) Gradual chemical reduction of GO: the band gap energy and schematic structure of rGO at various stages of the chemical reduction showing E_g changes from 3.5 to 1.0 eV [48]. Reprinted with permission from [48]. Copyright 2012 American Chemical Society. (b) Percentage of different carbon bonds as a function of GO thermal reduction obtained via XPS. Inset: sp^2 carbon and the corresponding oxygen concentration [49]. (c–f) Structural model of GO at various stages of thermal reduction: Lattice at (c) room temperature; (d) ~100°C; (e) ~220°C; and (f) ~500°C, where the dark gray area indicates sp^2 clusters and the light gray area represents sp^3 bonds to oxygen-containing groups [49]. Reprinted with permission from [49]. Copyright 2009 Wiley-VCH Verlag GmbH & Co. KGaA, Weinheim.

consideration, the thermal energy was shown to be very effective in the reduction of GO and the preparation of conductive film at the early stages (T < 700°C); even at excessive temperatures (T~1000°C), the entire sp^3 network cannot be eliminated and complete healing of the C–C bonds cannot be realized. From this result, Mattevi and coworkers [49] proposed a mechanistic model to describe the evolving conductive sp^2 network. As shown in **Figure 3c–f**, in the course of thermal reduction, the connection between the original conductive graphitic clusters (shown as dark gray in **Figure 3c**) is formed, which leads to development of the sp^2 network (**Figure 3d**). Electrical conductivity of polycrystalline graphite (1.25×10^3 S cm^{-1}) can be obtained at an sp^2 fraction of ~0.87 when a great portion of the sp^2 islands are connected via an sp^2 network (**Figure 3e**) and further enhanced up to the point that approaches the one for single-layer graphene (6×10^3 S cm^{-1}) at an sp^2 fraction of 0.95 (**Figure 3f**).

To accomplish a suitable band gap for solar water splitting and CO_2 reduction reactions, the graphene sp^2 network must be extensively interrupted by functionalization of various oxygenated groups. Thus, the interaction between molecular orbitals of carbon atoms and oxygen functionalities forms a forbidden electronic band as high as 2.7 eV, while maintaining sufficient carrier mobility to transfer the photo-induced charges. Crystalline defects create preferential bonding sites for the adsorption and deposition of atoms and molecules, which can be employed for the fabrication of interaction with active species in electrolyte. However, more

importantly, defects in the structure of graphene significantly enhance the density of dangling C—O bonds at the edges, which is very reactive for various redox reactions. The density of crystallographic defects must be optimized, as in contrast to aforementioned advantages; high density of structural defects increases the resistivity of graphene.

GO has exhibited photo-induced activity for reduction reactions by promoting electrons to their conduction band upon photon absorption. For example, GO was used for the UV-assisted reduction of biological samples (reduction of resazurin to resorufin), showing no sign of degradation at 350 nm [24]. Yeh et al. [50] investigated the functionality of GO for UV–Vis-induced sacrificial hydrogen evolution from 20% MeOH aqueous solution. Over the course of the reaction, in addition to the proton reduction at the active sites, evidently a portion of the photo-induced electrons interacted with the surface oxygen functional groups; thus, the band gap of the spent photocatalyst was reduced to 2.4 eV from its original 4.3 eV. Interestingly, the bare GO sample generated 17,000 μmol within 6 h under a 400 W high pressure mercury lamp, which was considered higher than the one loaded with 5 wt% Pt and far above the amount of hydrogen obtained from pure water (280 μmol) for the same period (**Figure 4a**). The low activity of the Pt-loaded sample is likely attributed to surface coverage of GO with opaque Pt nanoparticles.

GO has also exhibited visible-light (λ > 400 nm) activity in MeOH solution, as shown in **Figure 4b**, reached QE = 0.01%, which is significantly lower than that observed under a mercury lamp (QE = 2.70%). The stable evolution of hydrogen even at low band gap energy not only suggests that the CB of semiconducting GO is laid down at a suitable energy state corresponding to H^+/H_2 potential but also indicates that the transitional decay in the GO band gap is attributed to the upward shift of the VB, which is responsible for the lack of O_2 evolution, even in the presence of a scavenging Ag^+ ion [50]. This hypothesis can be extracted from the spectroscopic measurements, indicating that the removal of oxygen-containing groups on the surface leads to the reduction in the band gap through shifting the VB maximum upward, while the CB potential remained nearly unchanged at −0.75 to −0.71 eV versus Ag/AgCl [51, 52]. Further oxidization of GO increases the band gap and provides sufficient overpotential at the GO molecular orbital for an O_2 evolution reaction. However, the activity of the photocatalyst is expected to decline via photo-reduction, as shown for GO before and after photo reduction in **Figure 5a** and **b**, respectively [51].

The valence band maximum (VBM) and conduction band minimum (CBM) potential of GO can be tuned through doping, so within the localized sp^2 islands, both p- and n-type conductivities can be formed [30]. Therefore, individual islands may be activated for one photocatalytic half-reaction corresponding to their electrical characteristics. GO is intrinsically p-type due to electron-withdrawing oxygen functional groups on its surface [17]. Replacing these oxygen-containing groups with nitrogen, via noninvasive routes such as high temperature ammonolysis [53], results in n-type GO [30]. N-doped graphene oxide quantum dots (NGO–QDs) containing 6% carbon-bonding composition with N1 s/C1s = 2.9% posed a 2.2 eV band gap and exhibited overall water splitting under visible-light irradiation, comparable to that of the $Rh_{2-y}Cr_yO_3$ loaded GaN:ZnO solid solution photocatalyst, without the use of any precious metals [53]. The origin of this activity can be explained through the co-existence of p- and n-type conductivity within the lattice of

the N-doped graphene QDs divided by the original sp^2 islands (ohmic contacts). Thus, the photo-induced electrons and holes recombined at this contact, providing charges at suitable energy states for overall water splitting, is demonstrated in **Figure 6**.

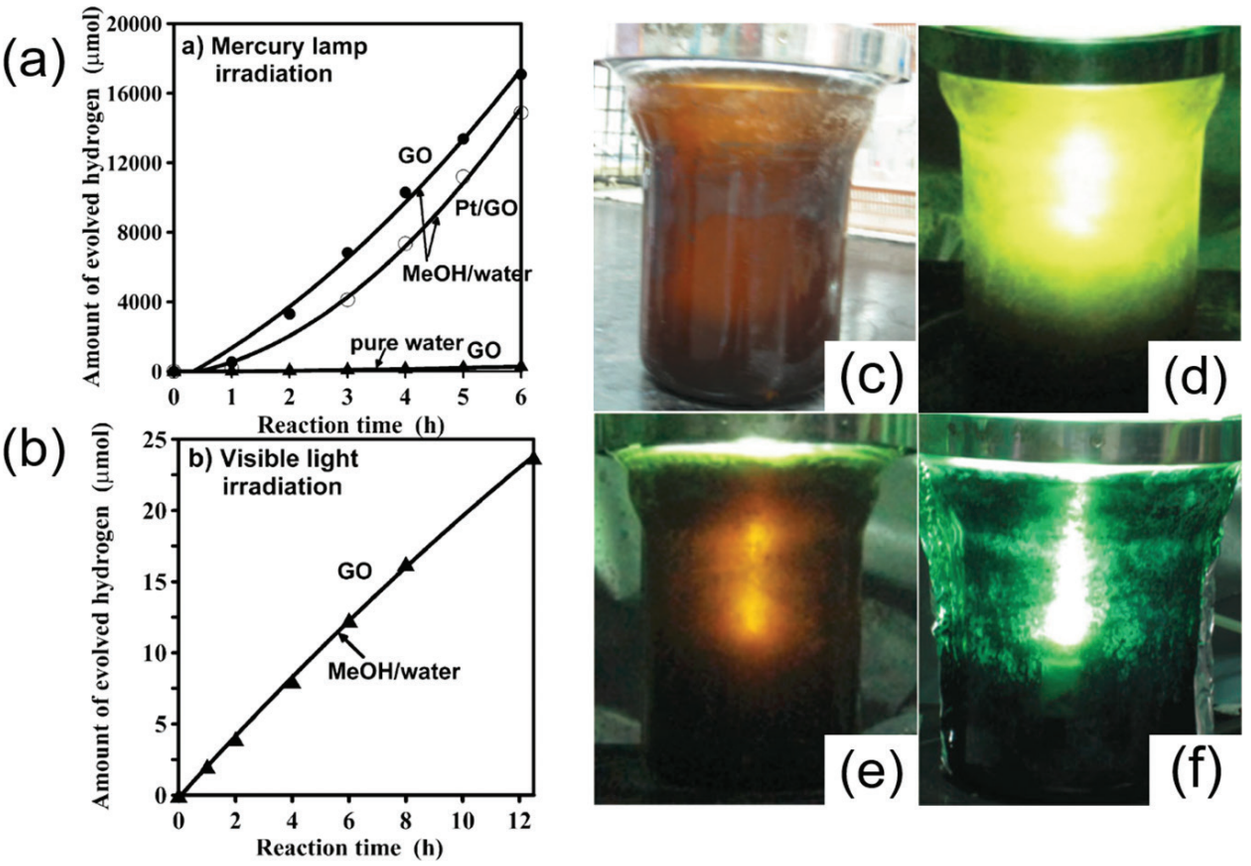

Figure 4. Hydrogen evolution from 20% MeOH solution and pure water using GO and 5 wt% Pt loaded GO photocatalysts (a) under UV–Vis irradiation and (b) under Vis irradiation. (c–f) Color variation of GO photocatalyst in a 20% MeOH solution indicating the self-reduction of GO (c) before irradiation; (d) at the start of irradiation; (e) after 30 min; and (f) after 2 h [50]. Reprinted with permission from [50]. Copyright 2010 Wiley-VCH Verlag GmbH & Co. KGaA, Weinheim.

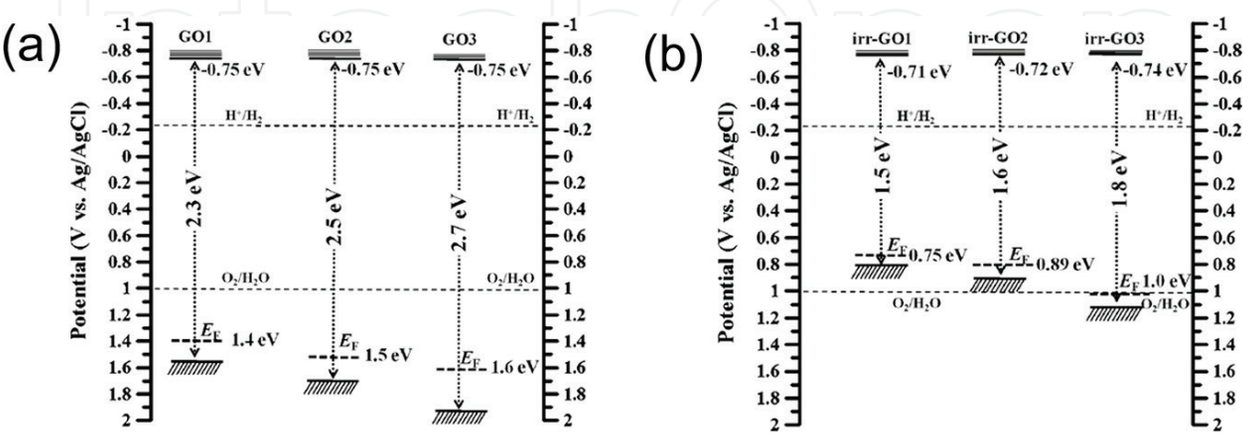

Figure 5. Band structure of GO samples (a) before and (b) after UV irradiation. GO1, GO2, and GO3 denoted for GO samples processed at oxidized through Hummers method for 4, 12, and 24 h [51]. Reprinted with permission from [51]. Copyright 2011 American Chemical Society.

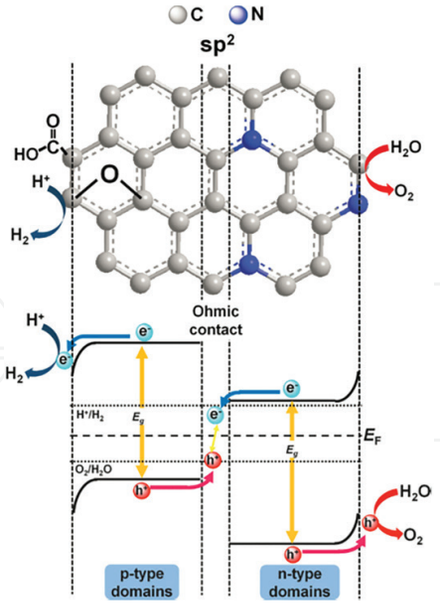

Figure 6. Mechanism of overall water splitting on p-type and n-type conductivity in GO lattice interconnected with sp^2 ohmic contact [53]. Reprinted with permission from [53]. Copyright 2014 Wiley-VCH Verlag GmbH & Co. KGaA, Weinheim.

Tan et al. [54], for the first time, reported the activity of isolated GO nanosheets for the conversion of CO_2 to methane (0.0628 μmol g^{-1} h^{-1} for 2 h) under visible light (15 W energy-saving daylight bulb source), although in situ photo-induced removal of oxygen functional groups resulted in a gradual decrease in methanol generation. CO_2 conversion to MeOH was also reported over modified graphene oxides with various band gap energies [55]. The phosphate-modified graphene with band gap ~3.2–4.4 eV produced methanol from CO_2 at 0.172 μmol gr^{-1} h^{-1}, nearly six times higher than the one measured for commercial TiO_2 under a 300 W halogen lamp. Since the photoexcitation in GO attributed to the surface oxygenated bonds, in this system, surface modification facilitated the electron/hole pair generation, which resulted in oxygen evolution and CO_2 reduction at the VB and CB, respectively [53].

Due to the high redox activity of crystalline defects in 2D carbon structures, graphene hybridized light absorber antenna have been the subject of photo-electro-chemical research. Dye sensitization has emerged as an effective technique to harvest a visible portion of the solar spectrum, and an alternative to the utilization of costly inorganic semiconductors [56–60]. A positive charge on the surface of dye molecules promotes their association and interfacial contact with negatively charged GO through electrostatic attraction. Latorre-Sánchez and coworkers [52] have functionalized the surface of GO with various degrees of oxidation (~10% carbon-oxygen content), hybridized it with a series of dye molecules (up to 39 wt%), and tested the fabricated composite for H_2 evolution in 20 V% methanol solution under 532 nm monochromatic light. In their experiment, the composite of cationic and anodic Ru dye complexes were anchored to the interlayer space of multilayer GO. The cationic $[Ru(bipy)_3]^{2+}$ exhibited the highest total corrected hydrogen evolution (with regard to dye absorption spectra), while the anodic Ru polypyridyl complex (N719) demonstrated the highest hydrogen evolution rate after nearly 100 min induction period. The induction period for N719 dye is likely attributed to the activation period, and/or the relocation

of dye molecules through the redox reaction. Pt-loaded rGO nanosheets as electron mediators for Eosin Y (EY) dye molecules has exhibited 9.3% QE under visible light, which is significantly greater than those recorded for EY-Pt and EY-rGO composites (**Figure 7a**). Due to the position of the energy bands, the excited electrons are transferred from the CB of the dye molecule to rGO and eventually to Pt active sires, as demonstrated in **Figure 7b**.

Further tailoring the band structure is shown to be highly effective, as the 5 wt% Pt-loaded GO nanosheets cosensitized by 1:1 M EY: Rose Bengal (RB) dye molecules reached quantum yield as high as 37.3% in 15 V% TEOA solution under two 450 W Xe lamps adjusted for 520 and 550 nm irradiation [62].

3.2. Graphene as electron acceptor

The process of transportation of an excited electron-hole pair from an emitter or "donor" to an absorbing medium, or "acceptor" is called nonradiative energy transfer (NRET). According to a study by Raja and coworkers, the rate of NRET in layered materials such as graphene and MoS_2 is a function of number of layers by comparing the decay rates of quantum dot fluorescence when the chromophores are placed on graphene and MoS_2 [63]. As illustrated with a gray line in **Figure 8a**, the population of charge carriers decays relatively slowly (a luminescence lifetime of 5 ns) in the absence of the acceptor parties (graphene and MoS_2). After planting QDs on 2D materials, due to high NRET rate, the photoluminescence (PL) lifetime decay decreased by an order of magnitude. Interestingly, their study indicates that the PL lifetime (inversely proportional to NRET rate) drops and increases by increasing the number of layers in graphene and MoS_2, respectively (**Figure 8b**). This finding confirms the strong electron acceptor role of graphene and provides hints for fabrication of highly efficient energy conversion/storage and optoelectronic devices.

In the first demonstration of graphene-based electron acceptors, Liu et al. [64] reported a solution-processable functionalized graphene electron-accepter with poly(3-octylthiophene) and poly(3-hexylthiophene) donor materials, reaching power conversion efficiency of 1.4% at 100 mW cm^{-2} AM 1.5G. In 2008, Williams et al. [65] discovered a room-temperature technique for the in situ reduction of GO via the transfer of electrons from semiconductor bulk to nanosheets.

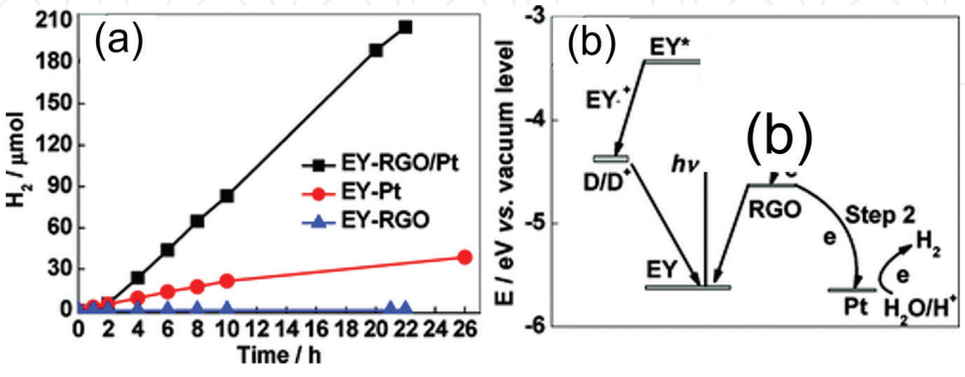

Figure 7. (a) The time courses of H_2 evolution over EY-Pt, EY-RGO, and EY-RGO-Pt photocatalysts and (b) photogenerated electron transfer from EY to rGO, and eventually to Pt, due to the composite energy level diagram [61]. Reprinted with permission from [61]. Copyright 2011 American Chemical Society.

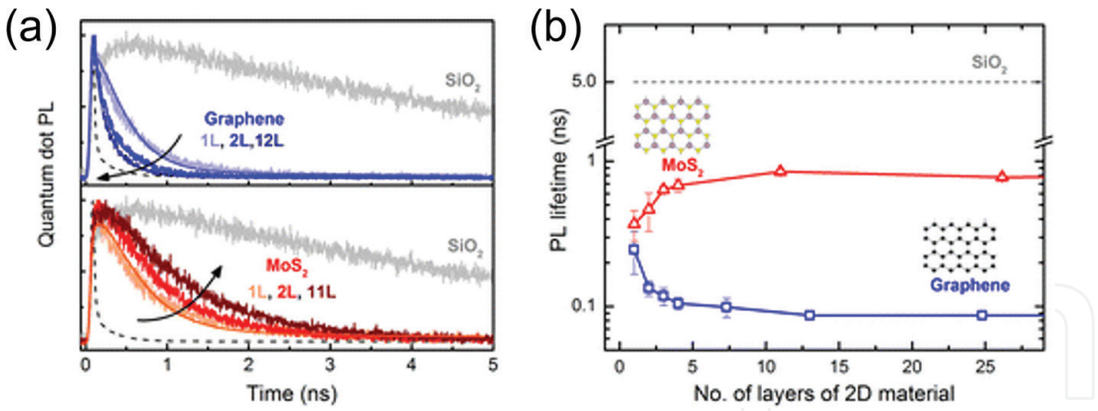

Figure 8. PL lifetime decay of QDs deposited on 2D graphene and MoS_2 (a) and the impact of graphene and MoS_2 thickness on the PL lifetime of charge carriers (b) [63]. Reprinted with permission from [63]. Copyright 2016 American Chemical Society.

This discovery facilitated the utilization of graphene derivatives as electron acceptors for solar fuel generation. The interesting work of Ng and coworkers [66] is one of the early studies of such efforts through the fabrication of $BiVO_4$ hybridized GO followed by in situ photo deposition.

In the last decade, various combinations of semiconductors and graphene-derivative electron acceptors and active sites were studied for effective solar fuel generation. Thus far, the combination of graphene derivatives and promising semiconducting photocatalyst via facile techniques was reported, including metal oxides [67–70], nitrides [71, 72], oxynitrides [26, 73], sulfides, and oxysulfides [74–77], as well as ternary composites [78] and those based on abundant Earth materials [79–81]. To realize the effectiveness of such hybridization, a recent study by Tang and coworkers [82] can be discussed. An advanced ternary photocatalytic system of TiO_2 nanotube-decorated CdS nanoparticles in composite with rGO nanosheets were synthesized and tested for photocatalytic hydrogen evolution where (1) the light absorption had been extended to the visible region; (2) the photo-excited charge separation significantly boosted and the electron path was configured to $CdS_{(CB)} \rightarrow TiO_{2(CB)} \rightarrow$rGO; and (3) CdS photo-corrosion was suppressed because of the rGO nanosheet protection (60 h stable H_2 evolution), via the so-called sheltering effect.

Readers are encouraged to read interesting review articles published recently on related topics, such as the one published by Xiang et al. [3] and Low et al. [6].

3.3. Graphene as electron mediator

Ternary nanocomposites of semiconductors and carbon-based materials can be designed and fabricated to tailor the absorption spectrum and to enhance the catalytic performance for solar fuel generation. The visible-light-responsive semiconductors were incorporated into the existing composites to further absorb the incident photons [82–85]. Effective electronic interaction between two photo-responsive components forms a recombination contact between the two and thus suppresses the unwanted recombination lost within one intrinsic component.

Hou et al. [78] reported an outstanding visible-light hydrogen evolution over the CdS-core TaON-shell rGO ternary composite prepared via the hydrothermal-assisted ion-exchange technique. In

this composite, rGO serves as an active site for H_2 evolution, as discussed in Section 3.1, as well as an electron mediator for efficient charge transfer within composite components. Due to the higher VB level of CdS, the photo-excited holes are promptly transferred to CdS and eventually to electrolyte and reduce the rate of recombination. By adding rGO and the Pt cocatalyst, the photo-induced electrons sink into rGO and subsequently into Pt, driven by their working function differentiation, which further reduces the recombination losses. The 1 wt% CdS-content ternary rGO hybridized core-shell composite decorated with 0.4% Pt reached 31% sacrificial apparent quantum efficiency at 420 nm (Na_2S-Na_2SO_3 aqueous solution), over twice that of the one without rGO and over 140 times of the bare TaON.

Z-scheme photocatalytic systems have demonstrated tremendous potential for efficient solar energy conversion. The first report on the stoichiometric water splitting into H_2 and O_2 through the Z-scheme mechanism was published in 1997 by Sayama et al. [86]. Since then, extensive studies have placed emphasis on the structure and catalytic behavior of individual Z-schematic components and their electronic interaction. Z-scheme water splitting is particularly of interest because the wide range of reduction and oxidation light-absorbing components provides design flexibilities for solar fuel generation. The conventional Z-scheme design is adapted through electron transfer from an O_2-evolving photocatalyst to an H_2-evolving photocatalyst via ionic electron mediators, such as IO^{3-}/I^- and Fe^{3+}/Fe^2 [87, 88]. Since the electron mediators must efficiently transfer electrons by adsorbing and desorbing onto and from the surfaces of photocatalysts, unstable semiconductors, such as metal sulfides, are not considered good candidates for Z-scheme water splitting [89]. Besides its role as an electron acceptor in semiconductor composites, graphene derivatives were used as a solid-state electron mediator for Z-scheme photocatalytic systems. Graphene-based compounds are excellent conductive platforms as solid-state electron mediators and provide enormous possibilities for the commercialization of Z-scheme solar-fuel-generation technology.

Recently, Iwashina et al. [89] synthesized a series of p-type metal sulfides (HER) in ternary composite with n-type rGO-TiO_2(OER). Among the various composites, $CuGaS_2$ loaded with 0.1 wt% Pt cocatalyst exhibited the highest activity for water splitting, yielding QE = 1.3% under 380 nm monochromatic irradiation. In this system, no appreciable gas evolution was observed in the absence of rGO, and/or either Pt-loaded $CuGaS_2$ or TiO_2, indicating the Z-schematic mechanism and the efficient contribution of rGO as an electron mediator.

The effectiveness of rGO as a solid-state electron mediator for Z-schematic water splitting consists of the $BiVO_4$ as O_2-evolution photocatalyst and Rh-doped $SrTiO_3$ decorated with Ru-complex cocatalyst [Ru(2,2′-bipyridine)(4,4′-diphosphonate-2,2′-bipyridine)$(CO)_2]^{2+}$ as H_2-evolving photocatalyst was investigated, as demonstrated in **Figure 9a**, which suggests enormous potential for electrolyte-independent overall water splitting [90, 91]. The electrons in the CB of $BiVO_4$ and the holes in the VB of $SrTiO_3$:Rh cannot meet the energy requirements for water reduction and oxidization, respectively. Therefore, as depicted in **Figure 9b**, upon visible light excitation, the electrons in the CB of $BiVO_4$ and the holes in the electron-donor level of $SrTiO_3$:Rh are transferred to the rGO mediator and recombined at the conductive support. The free electrons and holes on the $SrTiO_3$:Rh and $BiVO_4$ surface freely participated in the H_2 and O_2 evolution, respectively. Due to this effective electron mediator characteristic of rGO, as shown

in **Figure 9c**, the stoichiometric and stable visible-light driven Z-scheme overall water splitting for the $BiVO_4$-rGO-$SrTiO_3$:Rh decorated with Ru-based HER cocatalyst system was observed.

The complex catalysts based on ruthenium have been extensively studied due to their potential in mimicking the plant photosynthesis process [92]. In particular, Ru complexes demonstrated stable and promising performances for CO_2 conversion with high selectivity toward HCOOH [93]. The ruthenium complex reduction catalyst containing 2-thiophenyl benzimidazole ligands (schematic **Figure 10**) was studied for visible-light CO_2 reduction while it was covalently anchored to GO through the epoxide groups on the GO surface [94]. The treatment of GO with chloroacetic acid leads to conversion of the ─OH and epoxide groups to ─COOH groups, which was further treated by thionyl chloride to transform GO─COOH to ─COCl functionalized GO. This 2D platform is ideal for interaction with the Ru-complex, as schematically illustrated in **Figure 10**. The Ru-complex-GO composite produced over 2000 μmol g^{-1} of formic acid in 20 h, without use of a sacrificial reagent.

Kuai and coworkers [95] fabricated TiO_2–CdS encapsulated rGO composite where graphene was used as a solid-sate electron mediator for the Z-schematic conversion of CO_2 in the presence of water vapor. Hydrothermally prepared CdS nanospheres, as shown in **Figure 11a** and **b**, were positively charged and wrapped inside rGO nanosheets via self-assembly, which was induced by electrostatic forces (**Figure 11c** and **d**), followed by kinetic-controlled deposition of TiO_2 nanoparticles, as illustrated in **Figure 11e**. Such nanostructure is highly beneficial for Z-scheme photocatalysis, since rGO is positioned between two redox antenna/active sites, as demonstrated in **Figure 11f**, where ideal interfacial contact between the composite components can be maintained. Thus, the photo-induced electrons in TiO_2 CB are transferred to rGO and subsequently recombine with the holes generated at the CdS nanosphere's VB, resulting in enhanced density of photo-generated electrons and holes on the CdS nanosphere and TiO_2 nanoparticles, respectively. The photocatalytic efficiency of the CdS-rGO-TiO_2 Z-scheme system under 300 W Xe lamp irradiation was remarkably enhanced relative to pristine CdS, CdS-TiO_2, and CdS-rGO composites.

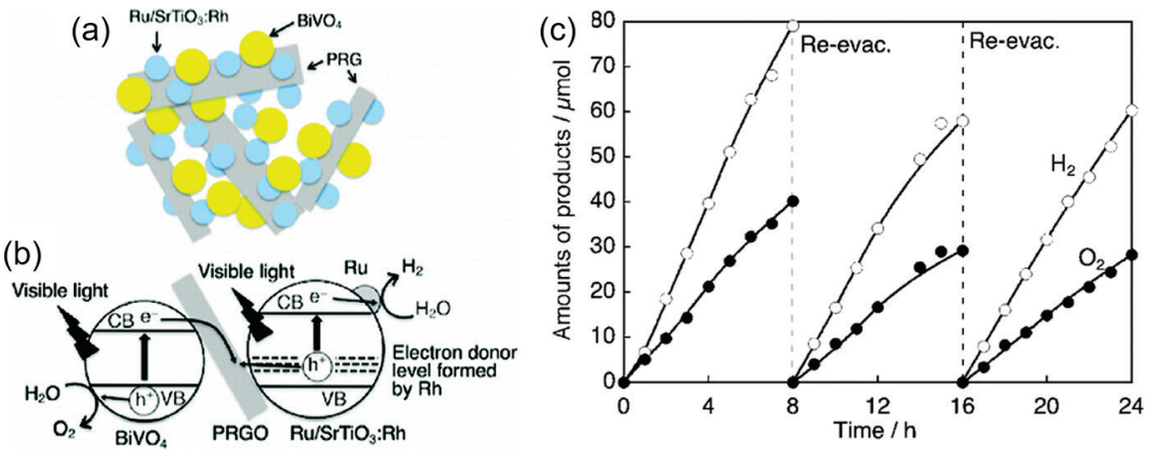

Figure 9. (a) Schematic illustration of rGO-mediated Z-scheme water splitting in Ru-SrTiO3:Rh (HER) and $BiVO_4$ (OER) system. (b) Photo-induced charge transfer driven by the energy band structure of the composite. (c) Time-course of visible light Z-scheme overall water splitting of Ru-$SrTiO_3$:Rh-rGO-$BiVO_4$ under a 300 W Xe lamp [90]. Reprinted with permission from [90]. Copyright 2011 American Chemical Society.

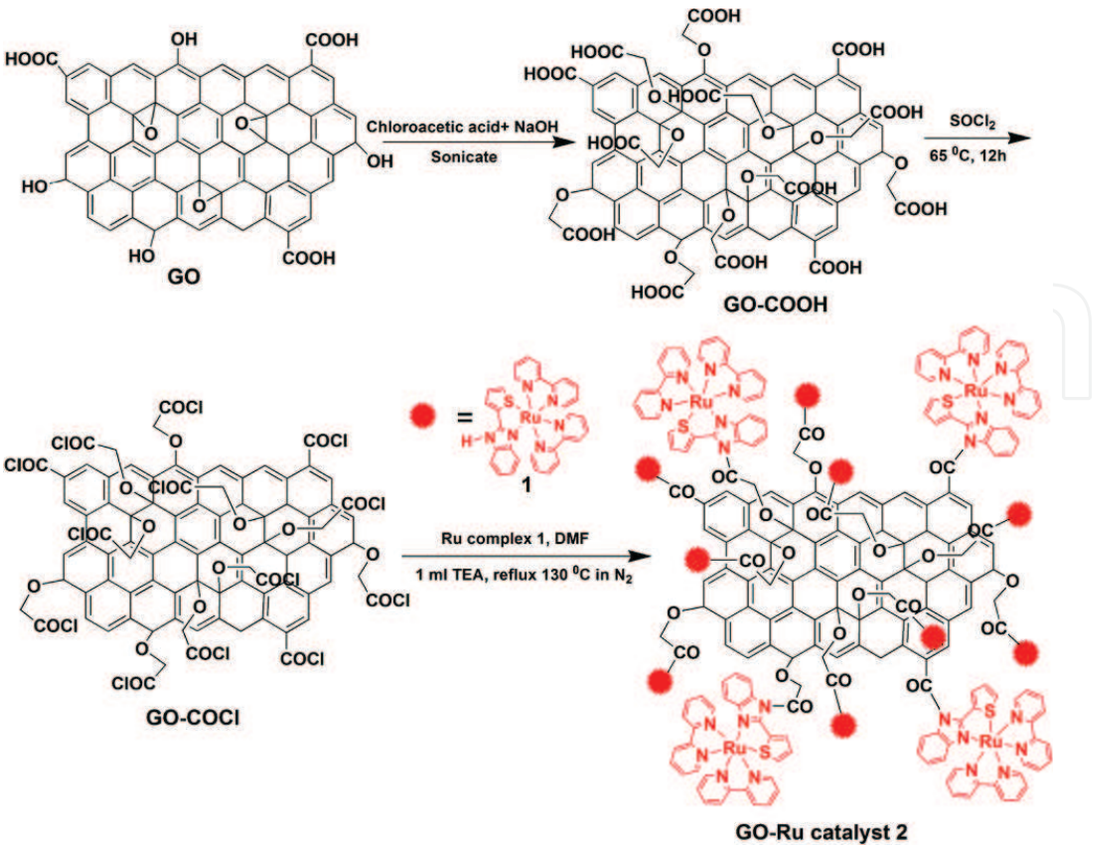

Figure 10. Surface functionalization of GO with a Ru catalyst complex [94]. Reprinted with permission from [94]. Copyright 2015 Royal Society of Chemistry.

3.4. Graphene as thermally-induced medium

Until now, the majority of studies on graphene-based photocatalysts have placed their focus on the role of graphene derivatives as transparent/flexible electrodes, electron acceptors, and electron mediators. Recently, the functionality of graphene-based compounds was investigated as a light absorber. In the recent years, it was concluded that graphene could absorb the entire solar spectrum because of its black color and zero band gap. Although such capability does not lead to active electron/hole pair generation for photocatalytic reaction, it does result in local high-temperature zones inside and on the surface of the photocatalyst, due to the photo-thermal effect, and enhances photocatalytic activity. According to a study by Gan and coworkers [96], such a photo-thermal effect contributes up to 38% in the photo-degradation of organic pollutants in the P25-rGO composite.

Colloidal QDs exhibit high quantum efficiencies through band gap engineering methods and are known to be excellent absorbers and emitters at various wavelengths [63]. Graphene QDs can be prepared via green and facile techniques [97], and have demonstrated strong quantum confinement at sizes below 10 nm [98]. The challenge of employing the interesting PL properties of graphene QDs for visible-light photocatalytic applications is their excitation-dependent PL properties, which means that at various excitation wavelengths, different energies are induced in the orbital structure of QDs. Zhuo et al. [98] prepared graphene QDs through the facile ultrasound route and exhibited an excitation-independent PL peak at 407 nm. Due to this constant PL emission, rutile

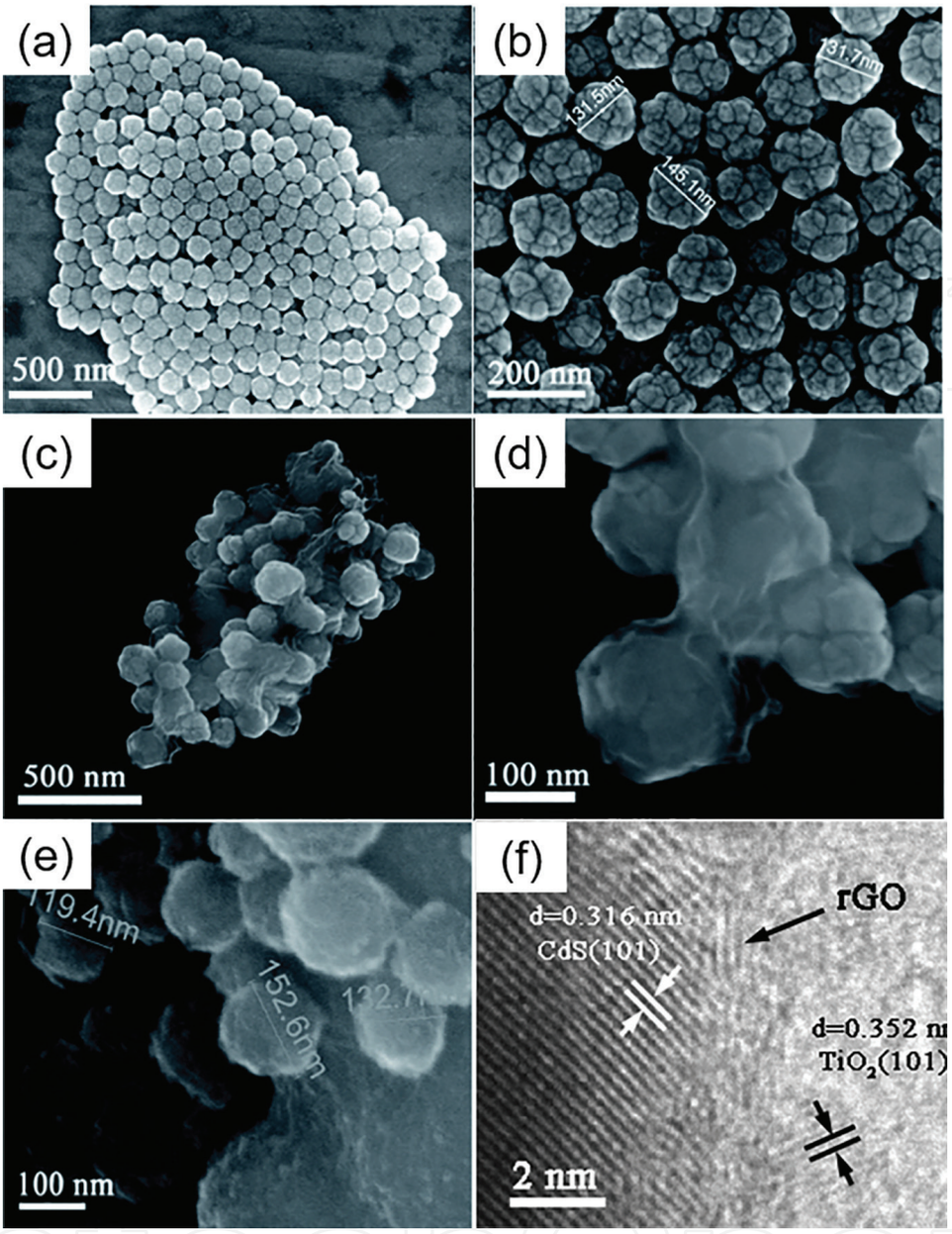

Figure 11. SEM images of CdS NSs (a and b), CdS NSs/GO (c and d), CdS NSs/rGO/TiO_2 (e) and the HRTEM image of CdS NSs/rGO/TiO_2 (f) [95]. Reprinted with permission from [95]. Copyright 2015 Royal Society of Chemistry.

TiO_2-QDs showed nine-fold visible-light catalytic activity (since it has a narrower band gap than 407 nm), compared to that of anatase TiO_2 (a band gap larger than 407 nm).

Recently, free-standing vertical graphene exhibited high potential as a light absorber. Zhao and coworkers [99] proposed a detailed mechanism for plasma-enhanced chemical vapor deposition of free-standing vertical graphene nanosheets, which is validated by transmission electron microscopy observations at the nucleation and growth stages. Davami et al. [100] reported that such morphology absorbs up to 97% of incident photons, which is much higher than previous carbon-based absorber materials, such as forest CNTs. Although free-standing graphene absorbers are yet to be studied for the solar-fuel-generation application, preliminary research data suggest their great potential for future-generation photocatalytic applications.

4. Conclusion and perspective

Graphene-derivatives, such as graphene oxide, reduced graphene oxide, and their functionalized materials are attractive components in optoelectronic device fabrication, owing to their peculiar optical, thermal, mechanical, and electrochemical properties. In particular, the 2D carbon nanostructure has proven to be an excellent candidate for the extraction of solar energy and its chemical transformation to fuel through photocatalytic water splitting and CO_2 conversion. Graphene derivatives' ultra-high specific surface area, which promotes the rate of redox reactions; its tunable band gap, which controls their absorption spectrum; its controllable defects density, which promotes their reactivity; and its carrier mobility, which promotes charge separation, all offer design flexibility at the nanoscale. However, the performance of graphene-based photocatalytic systems is vastly unpredictable, and understanding the role of graphene in photocatalytic fuel generation is still under debate. Over 18,000 articles related to graphene were published from 2004 to 2014. This rapid progress seeks continuous publication of critical reviews to genuinely add to the existing literature and to discuss the state-of-the-art development. Looking at the fast-paced advances in nanotechnology and materials sciences, it is apparent that the use of solar energy is an indispensable reality. The sunlight-induced splitting of waste water and atmospheric CO_2 reduction offers the onsite production of clean and renewable energy, as well as bacterial disinfection and pollutant decomposition. Therefore, the search for a highly active photocatalyst that can be produced through low-cost and scalable routes, exhibits a stable performance, and does not pose any threat to the environment is an extremely important task. Graphene derivatives are among the few candidates that meet all the aforementioned conditions.

Author details

Babak Adeli[1] and Fariborz Taghipour[1,2]*

*Address all correspondence to: fariborz.taghipour@ubc.ca

1 Photoreaction Engineering Laboratory, Chemical and Biological Engineering Department, University of British Columbia, Vancouver, BC, Canada

2 Clean Energy Research Centre (CERC), University of British Columbia, Vancouver, BC, Canada

References

[1] Adeli B, Taghipour FA. Review of synthesis techniques for gallium-zinc oxynitride solar-activated photocatalyst for water splitting. ECS Journal of Solid State Science and Technology. 2013;**2**:Q118-Q126

[2] Crabtree GW, Lewis NS. Solar energy conversion. Physics Today. 2007;**60**:37-42

[3] Xiang Q, Cheng B, Yu J. Graphene-based photocatalysts for solar-fuel generation. Angewandte Chemie International Edition. 2015;**54**:11350-11366

[4] Adeli B, Taghipour F. Facile synthesis of highly efficient nano-structured gallium zinc oxynitride solid solution photocatalyst for visible-light overall water splitting. Applied Catalysis A: General. 2016;**521**:250-258

[5] Huang X, Yin Z, Wu S, et al. Graphene-based materials: Synthesis, characterization, properties, and applications. Small. 2011;**7**:1876-1902

[6] Low J, Yu J, Ho W. Graphene-based Photocatalysts for CO2 reduction to solar fuel. Journal of Physical Chemistry Letters. 2015;**6**:4244-4251

[7] An X, Yu JC. Graphene-based photocatalytic composites. RSC Advances. 2011;**1**:1426

[8] Xiang Q, Yu J. Graphene-based photocatalysts for hydrogen generation. Journal of Physical Chemistry Letters. 2013;**4**:753-759

[9] Sun Y, Wu Q, Shi G. Graphene based new energy materials. Energy & Environmental Science. 2011;**4**:1113

[10] Novoselov KSS, Geim AKK, Morozov SVV, et al. Electric field effect in atomically thin carbon films. Science (80-). 2004;**306**:666-669

[11] Inagaki M, Kim Y a., Endo M. Graphene: Preparation and structural perfection. Journal of Materials Chemistry 2011;**21**:3280

[12] Hazra KS, Sion N, Yadav A, et al. Vertically aligned graphene based non-cryogenic bolometer. 2013. http://arxiv.org/abs/1301.1302 [Accessed: 12 July 2017]

[13] Garg R, Dutta NK, Choudhury NR. Work function engineering of graphene. Nanomaterials. 2014;**4**:267-300

[14] Miró P, Audiffred M, Heine T, et al. An atlas of two-dimensional materials. Chemical Society Reviews. 2014;**43**:6537-6554

[15] Huang X, Qi X, Boey F, et al. Graphene-based composites. Chemical Society Reviews. 2012;**41**:666-686

[16] Xiang Q, Yu J, Jaroniec M. Graphene-based semiconductor photocatalysts. Chemical Society Reviews. 2012;**41**:782

[17] Loh KP, Bao Q, Ang PK, et al. The chemistry of graphene. Journal of Materials Chemistry. 2010;**20**:2277

[18] Nair RR, Blake P, Grigorenko AN, et al. Fine structure constant defines visual transperency of graphene. Science (80-). 2008;**320**:2008

[19] Huang X, Zeng Z, Fan Z, et al. Graphene-based electrodes. Advanced Materials. 2012; **24**:5979-6004

[20] Chabot V, Higgins D, Yu A, et al. A review of graphene and graphene oxide sponge: Material synthesis and applications to energy and the environment. Energy & Environmental Science. 2014;**7**:1564

[21] Hsu HC, Shown I, Wei HY, et al. Graphene oxide as a promising photocatalyst for CO_2 to methanol conversion. Nanoscale. 2012;**5**:262-268

[22] Yeh TF, Cihlar J, Chang CY, et al. Roles of graphene oxide in photocatalytic water splitting. Materials Today. 2013;**16**:78-84

[23] Compton OC, Nguyen ST. Graphene oxide, highly reduced graphene oxide, and graphene: Versatile building blocks for carbon-based materials. Small. 2010;**6**:711-723

[24] Krishnamoorthy K, Mohan R, Kim S-J. Graphene oxide as a photocatalytic material. Applied Physics Letters. 2011;**98**:24-27

[25] Chen D, Feng H, Li J. Graphene oxide: Preparation, functionalization, and electrochemical applications. Chemical Reviews. 2012;**112**:6027-6053

[26] Adeli B, Taghipour F. Reduced graphene oxide composite of gallium zinc oxynitride photocatalyst with improved activity for overall water splitting. Chemical Engineering and Technology. 2016;**39**:142-148

[27] Ito J, Nakamura J, Natori A. Semiconducting nature of the oxygen-adsorbed graphene sheet. Journal of Applied Physics. 2008;**103**:113712

[28] Gao W. The chemistry of graphene oxide. Graphene Oxide: Reduction Recipes, Spectroscopy, and Applications. 2015;**39**:61-95

[29] Johari P, Shenoy VB. Modulating optical properties of graphene oxide: Role of prominent functional groups. ACS Nano. 2011;**5**:7640-7647

[30] Loh KP, Bao Q, Eda G, et al. Graphene oxide as a chemically tunable platform for optical applications. Nature Chemistry. 2010;**2**:1015-1024

[31] Pinto H, Jones R, Goss JP, et al. Unexpected change in the electronic properties of the au-graphene interface caused by toluene. Physical Review B: Condensed Matter and Materials Physics. 2010;**82**:1-8

[32] Yu S, Zhong Y-Q, B-Q Y, et al. Graphene quantum dots to enhance the photocatalytic hydrogen evolution efficiency of anatase TiO_2 with exposed {001} facet. Physical Chemistry Chemical Physics. 2016;**18**:20338-20344

[33] Yang KD, Ha Y, Sim U, et al. Graphene quantum sheet catalyzed silicon photocathode for selective CO_2 conversion to CO. Advanced Functional Materials. 2016;**26**:233-242

[34] Li L, Wu G, Yang G, et al. Focusing on luminescent graphene quantum dots: Current status and future perspectives. Nanoscale. 2013;**5**:4015

[35] Liu H, Liu Y, Zhu D. Chemical doping of graphene. Journal of Materials Chemistry. 2011; **21**:3335

[36] Lu G, Yu K, Wen Z, et al. Semiconducting graphene: Converting graphene from semimetal to semiconductor. Nanoscale. 2013;**5**:1353

[37] Avouris P. Graphene: Electronic and photonic properties and devices. Nano Letters. 2010;**10**:4285-4294

[38] Du A, Ng YH, Bell NJ, et al. Hybrid graphene/titania nanocomposite: Interface charge transfer, hole doping, and sensitization for visible light response. Journal of Physical Chemistry Letters. 2011;**2**:894-899

[39] Berger C, Song Z, Li X, et al. Electronic confinement and coherence in patterned epitaxial graphene. Science (80-). 2006;**312**:1191-1196

[40] Ando T. The electronic properties of graphene and carbon nanotubes. NPG Asia Materials. 2009;**1**:17-21

[41] Zhang X, Rajaraman BRS, Liu H, et al. Graphene's potential in materials science and engineering. RSC Advances. 2014;**4**:28987-29011

[42] Vicarelli L, Heerema SJ, Dekker C, et al. Controlling defects in graphene for optimizing the electrical properties of graphene nanodevices. ACS Nano. 2015;**9**:3428-3435

[43] Kim KS, Rhee KY, Park SJ. Influence of multi-walled carbon nanotubes on electrochemical performance of transparent graphene electrodes. Materials Research Bulletin. 2011;**46**:1301-1306

[44] Fan Z, Yan J, Zhi L, et al. A three-dimensional carbon nanotube/graphene sandwich and its application as electrode in supercapacitors. Advanced Materials. 2010;**22**:3723-3728

[45] Yu K, Lu G, Bo Z, et al. Carbon nanotube with chemically bonded graphene leaves for electronic and optoelectronic applications. Journal of Physical Chemistry Letters. 2011; **2**:1556-1562

[46] Velten J, Mozer AJ, Li D, et al. Carbon nanotube/graphene nanocomposite as efficient counter electrodes in dye-sensitized solar cells. Nanotechnology. 2012;**23**:85201

[47] Vempati S, Uyar T. Fluorescence from graphene oxide and the influence of ionic, π–π interactions and heterointerfaces: Electron or energy transfer dynamics. Physical Chemistry Chemical Physics. 2014;**16**:21183-21203

[48] Mathkar A, Tozier D, Cox P, et al. Controlled, stepwise reduction and band gap manipulation of graphene oxide. Journal of Physical Chemistry Letters. 2012;**3**:986-991

[49] Mattevi C, Eda G, Agnoli S, et al. Evolution of electrical, chemical, and structural properties of transparent and conducting chemically derived craphene thin films. Advanced Functional Materials. 2009;**19**:2577-2583

[50] Yeh T-F, Syu J-M, Cheng C, et al. Graphite oxide as a photocatalyst for hydrogen production from water. Advanced Functional Materials. 2010;**20**:2255-2262

[51] Yeh TF, Chan FF, Hsieh C, Te, et al. Graphite oxide with different oxygenated levels for hydrogen and oxygen production from water under illumination: The band positions of graphite oxide. Journal of Physical Chemistry C. 2011;**115**:22587-22597

[52] Latorre-Sánchez M, Lavorato C, Puche M, et al. Visible-light photocatalytic hydrogen generation by using dye-sensitized graphene oxide as a photocatalyst. Chemistry: A European Journal. 2012;**18**:16774-16783

[53] Yeh TF, Teng CY, Chen SJ, et al. Nitrogen-doped graphene oxide quantum dots as photocatalysts for overall water-splitting under visible light illumination. Advanced Materials. 2014;**26**:3297-3303

[54] Tan L-L, Ong W-J, Chai S-P, et al. Reduced graphene oxide-TiO_2 nanocomposite as a promising visible-light-active photocatalyst for the conversion of carbon dioxide. Nanoscale Research Letters. 2013;**8**:465

[55] Hsu H-C, Shown I, Wei H-Y, et al. Graphene oxide as a promising photocatalyst for CO_2 to methanol conversion. Nanoscale. 2013;**5**:262-268

[56] Choi SK, Yang HS, Kim JH, et al. Organic dye-sensitized TiO_2 as a versatile photocatalyst for solar hydrogen and environmental remediation. Applied Catalysis B: Environmental. 2012;**121-122**:206-213

[57] Choi SK, Kim S, Ryu J, et al. Titania nanofibers as a photo-antenna for dye-sensitized solar hydrogen. Photochemical & Photobiological Sciences. 2012;**11**:1437

[58] Tong L, Iwase A, Nattestad A, et al. Sustained solar hydrogen generation using a dye-sensitised NiO photocathode/$BiVO_4$ tandem photo-electrochemical device. Energy & Environmental Science. 2012;**5**:9472

[59] Gao Y, Ding X, Liu J, et al. Visible light driven water splitting in a molecular device with unprecedentedly high photocurrent density. Journal of the American Chemical Society. 2013;**135**:4219-4222

[60] Ding X, Gao Y, Zhang L, et al. Visible light-driven water splitting in photoelectrochemical cells with supramolecular catalysts on photoanodes. ACS Catalysis. 2014;**4**:2347-2350

[61] Min S, Lu G. Dye-sensitized reduced graphene oxide photocatalysts for highly efficient visible-light-driven water reduction. Journal of Physical Chemistry C. 2011; **115**:13938-13945

[62] Min S, Lu G. Dye-cosensitized graphene/Pt photocatalyst for high efficient visible light hydrogen evolution. International Journal of Hydrogen Energy. 2012;**37**:10564-10574

[63] Raja A, Montoya-Castillo A, Zultak J, et al. Energy transfer from quantum dots to graphene and MoS_2 : The role of absorption and screening in two-dimensional materials. Nano Letters. 2016;**16**:2328-2333

[64] Liu Z, Liu Q, Huang Y, et al. Organic photovoltaic devices based on a novel acceptor material: Graphene. Advanced Materials. 2008;**20**:3924-3930

[65] Williams G, Seger B, Kamt PV. TiO_2-graphene nanocomposites. UV-assisted photocatalytic reduction of graphene oxide. ACS Nano. 2008;**2**:1487-1491

[66] Ng YH, Iwase A, Kudo A, et al. Reducing graphene oxide on a visible-light $BiVO_4$ photocatalyst for an enhanced photoelectrochemical water splitting. Journal of Physical Chemistry Letters. 2010;**1**:2607-2612

[67] Xiang Q, Yu J, Jaroniec M. Enhanced photocatalytic H_2-production activity of graphene-modified titania nanosheets. Nanoscale. 2011;**3**:3670-3678

[68] Kim H, Moon G, Monllor-Satoca D, et al. Solar photoconversion using graphene/TiO_2 composites: Nanographene shell on TiO_2 core versus TiO_2 nanoparticles on graphene sheet. Journal of Physical Chemistry C. 2012;**116**:1535-1543

[69] Wang Y, Yu J, Xiao W, et al. Microwave-assisted hydrothermal synthesis of graphene based Au–TiO_2 photocatalysts for efficient visible-light hydrogen production. Journal of Materials Chemistry A. 2014;**2**:3847

[70] Zang Y, Li L, Zuo Y, et al. Facile synthesis of composite g-C_3N_4/WO_3: A nontoxic photocatalyst with excellent catalytic activity under visible light. RSC Advances. 2013;**3**:13646

[71] Ong W-J, Tan L-L, Chai S-P, et al. Surface charge modification via protonation of graphitic carbon nitride (g-C_3N_4) for electrostatic self-assembly construction of 2D/2D reduced graphene oxide (rGO)/g-C_3N_4 nanostructures toward enhanced photocatalytic reduction of carbon dioxide to methane. Nano Energy. 2015;**13**:757-770

[72] Xiang Q, Yu J, Jaroniec M. Preparation and enhanced visible-light photocatalytic H_2-production activity of graphene/C_3N_4 composites. Journal of Physical Chemistry C. 2011;**115**:7355-7363

[73] Mukherji A, Seger B, GQ L, et al. Nitrogen doped $Sr_2Ta_2O_7$ coupled with graphene sheets as photocatalysts for increased photocatalytic hydrogen production. ACS Nano. 2011;**5**:3483-3492

[74] Li Q, Guo B, Yu J, et al. Highly efficient visible-light-driven photocatalytic hydrogen production of CdS-cluster-decorated graphene nanosheets. Journal of the American Chemical Society. 2011;**133**:10878-10884

[75] Jia L, Wang DH, Huang YX, et al. Highly durable N-doped graphene/CdS nanocomposites with enhanced photocatalytic hydrogen evolution from water under visible light irradiation. Journal of Physical Chemistry C. 2011;**115**:11466-11473

[76] Xu J, Wang L, Cao X. Polymer supported graphene-CdS composite catalyst with enhanced photocatalytic hydrogen production from water splitting under visible light. Chemical Engineering Journal. 2016;**283**:816-825

[77] Chang CJ, Chu KW, Hsu MH, et al. Ni-doped ZnS decorated graphene composites with enhanced photocatalytic hydrogen-production performance. International Journal of Hydrogen Energy. 2015;**40**:14498-14506

[78] Hou J, Wang Z, Kan W, et al. Efficient visible-light-driven photocatalytic hydrogen production using CdS@TaON core–shell composites coupled with graphene oxide nanosheets. Journal of Materials Chemistry. 2012;**22**:7291

[79] Fan L, Liu PF, Yan X, et al. Atomically isolated nickel species anchored on graphitized carbon for efficient hydrogen evolution electrocatalysis. Nature Communications. 2016; **7**:10667

[80] Kibsgaard J, Jaramillo TF. Molybdenum phosphosulfide: An active, acid-stable, earth-abundant catalyst for the hydrogen evolution reaction. Angewandte Chemie International Edition. 2014;**53**:14433-14437

[81] McKone JR, Sadtler BF, Werlang CA, et al. Ni-Mo nanopowders for efficient electrochemical hydrogen evolution. ACS Catalysis. 2013;**3**:166-169

[82] Tang Y, Hu X, Liu C. Perfect inhibition of CdS photocorrosion by graphene sheltering engineering on TiO_2 nanotube array for highly stable photocatalytic activity. Physical Chemistry Chemical Physics. 2014;**16**:25321-25329

[83] Li H, Xia Z, Chen J, et al. Constructing ternary CdS/reduced graphene oxide/TiO_2 nanotube arrays hybrids for enhanced visible-light-driven photoelectrochemical and photocatalytic activity. Applied Catalysis B: Environmental. 2015;**168-169**:105-113

[84] Lin X, Wang Y, Zheng J, et al. Graphene quantum dot sensitized leaf-like $InVO_4$/$BiVO_4$ nanostructure: A novel ternary heterostructured QD-RGO/$InVO_4$/$BiVO_4$ composite with enhanced visible-light photocatalytic activity. Dalton Transactions. 2015;**44**:19185-19193

[85] Zhou J, Tian G, Chen Y, et al. In situ controlled growth of $ZnIn_2S_4$ nanosheets on reduced graphene oxide for enhanced photocatalytic hydrogen production performance. Chemical Communications. 2013;**49**:2237-2239

[86] Sayama K, Yoshida R, Kusama H, et al. Photocatalytic decomposition of water into H_2 and O_2 by a two-step photoexcitation reaction using a WO_3 suspension catalyst and an Fe^{3+}/Fe^{2+} redox system. Chemical Physics Letters. 1997;**277**:387-391

[87] Maeda K, Higashi M, Lu D, et al. Efficient nonsacrificial water splitting through two-step photoexcitation by visible light using a modified oxynitride as a hydrogen evolution photocatalyst. Journal of the American Chemical Society. 2010;**132**:5858-5868

[88] Sasaki Y, Iwase A, Kato H, et al. The effect of co-catalyst for Z-scheme photocatalysis systems with an Fe^{3+}/Fe^{2+} electron mediator on overall water splitting under visible light irradiation. Journal of Catalysis. 2008;**259**:133-137

[89] Iwashina K, Iwase A, Ng YH, et al. Z-schematic water splitting into H_2 and O_2 using metal sulfide as a hydrogen-evolving photocatalyst and reduced graphene oxide as a solid-state electron mediator. Journal of the American Chemical Society. 2015;**137**:604-607

[90] Iwase A, Ng YH, Ishiguro Y, et al. Reduced graphene oxide as a solid-state electron mediator in Z-scheme photocatalytic water splitting under visible light. Journal of the American Chemical Society. 2011;**133**:11054-11057

[91] Suzuki TM, Iwase A, Tanaka H, et al. Z-scheme water splitting under visible light irradiation over powdered metal-complex/semiconductor hybrid photocatalysts mediated by reduced graphene oxide. Journal of Materials Chemistry A. 2015;**3**:13283-13290

[92] Duan L, Bozoglian F, Mandal S, et al. A molecular ruthenium catalyst with water-oxidation activity comparable to that of photosystem II. Nature Chemistry. 2012;**4**:418-423

[93] Sato S, Morikawa T, Saeki S, et al. Visible-light-induced selective CO_2 reduction utilizing a ruthenium complex electrocatalyst linked to a p-type nitrogen-doped Ta_2O_5 semiconductor. Angewandte Chemie International Edition. 2010;**49**:5101-5105

[94] Kumar P, Bansiwal A, Labhsetwar N, et al. Visible light assisted photocatalytic reduction of CO_2 using a graphene oxide supported heteroleptic ruthenium complex. Green Chemistry. 2015;**17**:1605-1609

[95] Kuai L, Zhou Y, Tu W, et al. Rational construction of a CdS/reduced graphene oxide/TiO_2 core–shell nanostructure as an all-solid-state Z-scheme system for CO_2 photoreduction into solar fuels. RSC Advances. 2015;**5**:88409-88413

[96] Gan Z, Wu X, Meng M, et al. Photothermal contribution to enhanced photocatalytic performance of graphene-based nanocomposites. ACS Nano. 2014;**8**:9304-9310

[97] Ali J, Siddiqui G, Yang YJ, et al. Direct synthesis of graphene quantum dots from multilayer graphene flakes through grinding assisted co-solvent ultrasonication for all-printed resistive switching arrays. RSC Advances. 2016;**6**:5068-5078

[98] Zhuo S, Shao M, Lee S-T. Upconversion and downconversion fluorescent graphene quantum dots: Ultrasonic preparation and photocatalysis. ACS Nano. 2012;**6**:1059-1064

[99] Zhao J, Shaygan M, Eckert J, et al. A growth mechanism for free-standing vertical graphene. Nano Letters. 2014;**14**:3064-3071

[100] Davami K, Cortes J, Hong N, et al. Vertical graphene sheets as a lightweight light absorber. Materials Research Bulletin. 2016;**74**:226-233

IntechOpen